Propagation of Statistical Uncertainties of Skyrme Mass Models to Simulations of r-Process Nucleosynthesis

T.M. Sprouse,[1] R. Navarro Perez,[2] R. Surman,[1] M.R. Mumpower,[3] G.C. McLaughlin,[4] and N. Schunck[5]

[1]*Department of Physics, University of Notre Dame, Notre Dame, IN 46556, USA*
[2]*Department of Physics, San Diego State University, San Diego, CA 02182, USA*
[3]*Theoretical Division, Los Alamos National Laboratory, Los Alamos, NM 87545, USA*
[4]*Department of Physics, North Carolina State University, Raleigh, NC*
[5]*Nuclear and Chemical Science Division, Lawrence Livermore National Laboratory, Livermore, California 94551, USA*
(Dated: January 30, 2019)

Uncertainties in nuclear models have a major impact on simulations that aim at understanding the origin of heavy elements in the universe through the rapid neutron capture process (r process) of nucleosynthesis. Within the framework of the nuclear density functional theory, we use results of Bayesian statistical analysis to propagate uncertainties in the parameters of energy density functionals to the predicted r-process abundance pattern, by way not only of the nuclear masses but also through the influence of the masses on β-decay and neutron capture rates. We additionally make the first identifications of specific parameters of Skyrme-like energy density functionals which are correlated with particular aspects of the r-process abundance pattern. While previous studies have explored the reduction in the abundance pattern uncertainties due to anticipated new measurements of neutron-rich nuclei, here we point out that an even larger reduction will occur when these new measurements are used to reduce the uncertainty of model predictions of masses, which are then propagated through to the abundance pattern. We make a quantitative prediction for how large this reduction will be.

The heaviest elements owe their origins to rapid neutron capture, or r-process, nucleosynthesis. In the r-process, heavy elements are built up via a sequence of rapid neutron captures and β-decays that populate nuclei far to the neutron-rich side of stability [1, 2]. The astrophysical source of the intense neutron flux was initially suspected to be within core-collapse supernovae [3, 4], though decades of careful study have shown the required conditions are unlikely to be obtained in this environment [5–8]. Recent evidence [9, 10], including the discovery of GW170817/GRB170817a/SSS17a [11, 12], increasingly points to neutron star mergers as the likely r-process site. However, many open questions remain. For example, what specific environments within neutron star merger events are responsible for r-process production, and what are their properties? Can neutron star mergers account for all galactic r-process production, or are there additional astrophysical sites?

The r-process astrophysical conditions could in principle be identified by comparing simulations of abundance patterns of elements and observations in the solar system and in old stars. However, analysis of individual environments is complicated by large uncertainties in the astrophysics and nuclear physics [13]. Here we consider the latter. Simulations of the r-process are dependent upon nuclear data, including masses, neutron capture rates, and β-decay and fission properties, for thousands of neutron-rich nuclei [14]. In spite of a concerted effort at radioactive beam facilities worldwide to measure these properties directly or indirectly, the vast majority of them are as of yet inaccessible and we must rely on theoretical estimates.

Nuclear density functional theory (DFT) is currently the only approach that can provide all of these properties in a consistent yet microscopic framework [15]. Most energy density functionals (EDF) are typically characterized by approximately a dozen parameters that are fitted on a small set of nuclear properties. The choices made in selecting the form of the EDF and the set of experimental data to fit its parameters lead to both systematic and statistical uncertainties that have an impact on all applications [16].

Ideally, one would like to consider simultaneously all sources of uncertainties (systematic, statistical and numerical) and propagate them to all observables (separation energies, α-, β- and γ-decay rates, fission rates, neutron capture rates) relevant to astrophysical simulations. Such an approach is currently not feasible, partly because of its formidable computational cost, partly because there are still gaps in our understanding of, e.g., α-decay, neutron capture or fission. However, we can exploit recent work in determining estimates of theoretical uncertainties to quantify the variations in simulated r-process abundances that result from nuclear mass uncertainties alone. Past work in this area has either considered abundance pattern comparisons between distinct mass models, e.g. [17], or ranges of patterns that result from random, uncorrelated mass variations [14, 18].

In this work, we perform the first rigorous propagation of statistical uncertainties of nuclear mass models based on DFT. We generate fifty different EDFs by sampling the Bayesian posterior distribution of the UNEDF1 EDF.

For each sample, we compute a full nuclear chart and update neutron capture rates and β-decay properties to be consistent with each table. We implement these sets of nuclear data in r-process simulations to place "error bars" due to nuclear masses on r-process abundances and to identify correlations between theoretical model parameters and abundance pattern features. Such correlations could possibly lead to additional constraints on r-process conditions or, e.g., the UNEDF1 parameters themselves. Finally, we provide a quantitative estimate of the improvements to r-process pattern uncertainties expected from anticipated mass measurements at current and upcoming facilities and concurrent advancements in theoretical models.

We begin by computing atomic mass tables within the nuclear DFT approach to nuclear structure with Skyrme EDFs. Our starting point is the UNEDF1 parametrization, in which the coupling constants were optimized globally on select experimental nuclear masses, radii, deformations and excitation energies of fission isomers in the actinides [19]. While the r.m.s. deviation on nuclear binding energies of UNEDF1 is only 1.8 MeV, it goes down to 0.45 MeV for 2-neutron separation energies. Bayesian inference methods were later used to compute the posterior distribution of the UNEDF1 parameters [20] and propagate theoretical statistical uncertainties in predictions of nuclear masses, two-neutron drip line, and fission barriers [21]. Here, we sample the same posterior distribution within the 90% confidence region to generate fifty different parameter sets for the Skyrme EDF.

For each sample, we compute the nuclear ground-state binding energy of all even-even nuclei from Hydrogen to $Z = 120$ by solving the Hartree-Fock-Bogoliubov (HFB) equation. The limits of nuclear stability (proton and neutron drip lines) are reached when the value of the two neutron (proton) separation energy becomes negative. Compared to alternative options based, e.g., on the value of the Fermi energy, this criterion offers the advantage of being model-independent since binding energies are true observables. With this criterion, each mass table contains approximately 2,000 even-even nuclei. For each even-even nucleus, the ground-state is determined by exploring locally the potential energy surface of the nucleus for a range of eleven axial quadrupole deformations β_2 between -0.5 and +0.5. The configuration with the lowest energy defines the ground-state. Details of the exploration of the even-even nuclear landscape with the numerical solver HFBTHO can be found in [22]. With this procedure, computing 50 mass tables requires of the order of 1 million HFB calculations.

Although odd-even and odd-odd binding energies could be computed with the blocking procedure, see, e.g. [23], this would require about an order of magnitude more HFB calculations. Instead we adopt a standard approximation for the binding energy of odd nuclei that combines information about binding energies and HFB pairing gaps in neighboring isotopes/isotones; see Supplemental Material of [24]. This procedure yields an excellent approximation of, in particular, one-particle separation energies.
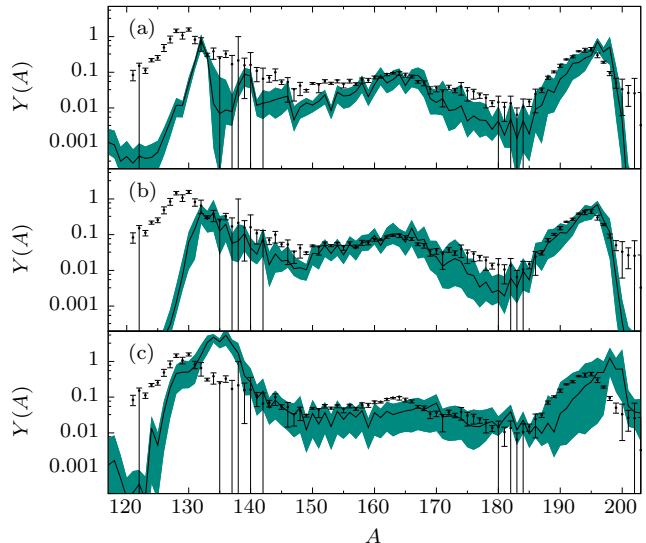

FIG. 1: Abundance patterns $Y(A)$ versus A for fifty r-process simulations with astrophysical conditions corresponding to high-entropy (top panel, (a)), low-entropy (middle panel, (b)), and fission-recycling (bottom panel, (c)) outflows, as described in the text. The shaded region shows the full range of abundance patterns produced, and the black line shows their mean. All patterns are scaled to solar abundances from [13].

For each of the fifty mass tables thus described, we calculate a self-consistent set of all nuclear data inputs required for r-process calculations. We calculate neutron capture and neutron-induced fission rates using the Los Alamos Hauser-Feshbach code CoH [25] and β-decay half-lives with probabilities for delayed emission of one or more neutrons using the QRPA+HF framework of [26] and unmodified strength data from [27]. We repeat these calculations using the masses given in the 2016 Atomic Mass Evaluation (AME2016) [28]; where possible, these results are taken to replace those based on the UNEDF1 mass tables. The decay properties of the Nubase 2016 compilation [29] are further taken to replace any calculated values based on either AME2016 or UNEDF1 nuclear masses. For all fissioning nuclei, we use a symmetric, two-particle product distribution.

We implement each of these datasets into the nuclear reaction network code PRISM [30–32] to simulate nucleosynthesis for three distinct types of astrophysical conditions where r-process nucleosynthesis may occur: (1) a supernova-type high-entropy wind, with entropy $s/k = 300$, dynamical timescale $\tau = 80$ ms, and electron fraction $Y_e = 0.30$, (2) a parameterized merger accretion disk wind with $s/k = 30$, $\tau = 80$ ms, and $Y_e = 0.21$, and

(3) fission-recycling outflow from a neutron star merger [33]. For each simulation, we dynamically update the evolution of temperature with respect to the release of energy from nuclear reactions, decays, and fission, with an assumed thermalization efficiency of 10% for all energy released.

The range in final abundance patterns across these fifty calculations is shown in Fig. 1 for each set of astrophysical conditions we consider. In each case, the shaded band represents the propagation of statistical uncertainties from the UNEDF1 nuclear mass model to the corresponding r-process simulation. The influence of masses on reaction and decay rates contribute to the width of the band, via mechanisms described in, e.g., [14] and references therein. In addition, the location of the neutron drip line is of key importance for some types of astrophysical conditions. In the fifty mass tables considered here, the location of the one-neutron drip line varies by more than ten neutron numbers. Notably, the band is the widest for the astrophysical conditions in which the r-process path is the closest to the drip line, the fission recycling example of Fig. 1(c).

With the wealth of data available from these r-process simulations, we can search for correlations between UNEDF1 functional parameters and the formation of abundance pattern features. Here we demonstrate how such analyses might proceed.

Several of the UNEDF1 functional parameters are poorly constrained by data near stability. One such parameter is the isovector surface coupling constant $C_1^{\rho\Delta\rho}$, with UNEDF1 value -145.382 ± 52.169; see Table II in [19]. For a low-entropy hot wind r-process environment, this parameter is correlated with the formation of the rare earth peak, the small feature around $A \sim 160$ in the solar r-process isotopic pattern. The top panel of Fig. 2 shows $C_1^{\rho\Delta\rho}$ versus the abundance-weighted average A of the rare earth peak for the r-process simulations from the middle panel of Fig. 1. The placement of the rare earth peak is calculated from the solar r-process abundances of [13] and [34] and is given by the shaded vertical band. Correlations between $C_1^{\rho\Delta\rho}$ and rare earth peak placement are weaker for other types of r-process environments. The r-process path in the high-entropy wind case is not so neutron-rich and thus not as sensitive to $C_1^{\rho\Delta\rho}$. The fission recycling example has a distinct rare earth peak formation mechanism [35] that is not particularly active with the UNEDF1 masses, resulting in a comparatively weaker correlation. However, recent studies [36–41] favor r-process conditions that are most similar to those of our low-entropy wind where this correlation is strongest, suggesting that the r-process abundance pattern may provide an important additional constraint on the value of $C_1^{\rho\Delta\rho}$.

In all of the astrophysical environments considered, we found the proton pairing strength V_0^p to be correlated with the ratio between the summed abundances of the
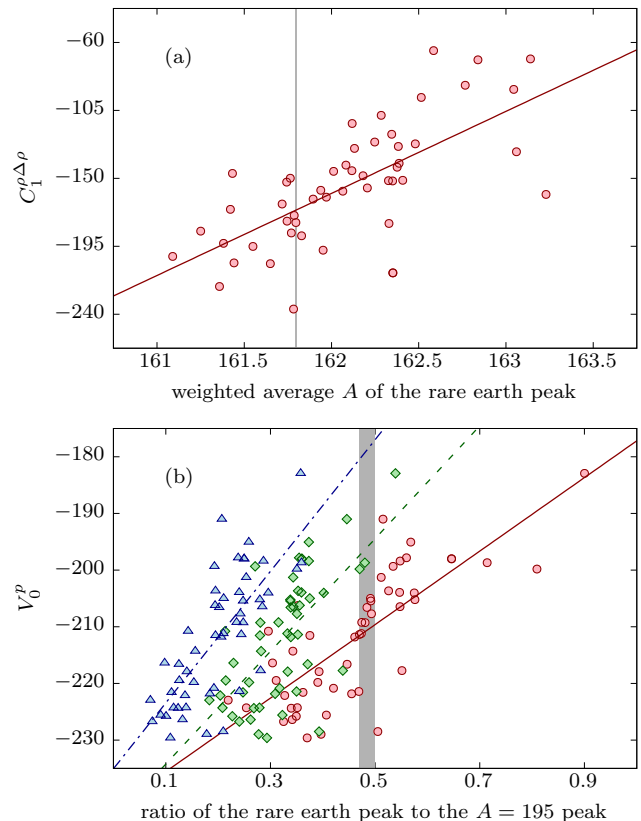

FIG. 2: Relationship between r-process abundance pattern and UNEDF1 functional parameters for fifty UNEDF1 mass tables. Panel (a) shows the relationship between the weighted average mass number A of the rare earth peak and the isovector surface coupling constant $C_1^{\rho\Delta\rho}$ for the low-entropy wind conditions of Fig. 1. A linear fit to the dataset is given by the solid line with correlation coefficient $r = 0.68$. Panel (b) shows the relationship between the proton pairing strength V_0^p and the ratio of summed abundances in the rare earth region to the $A = 195$ region for the high-entropy (green diamonds), low-entropy (red circles), and fission recycling (blue triangles) conditions from Fig. 1, with linear fits given for the high-entropy dataset by the green dashed line ($r = 0.66$), the low-entropy dataset by the red solid line ($r = 0.76$), and the fission recycling dataset by the blue dot-dashed line ($r = 0.75$). The gray shaded region in each figure indicates the range of values in each metric admitted by the solar abundances of [13] and [34].

rare earth and $A \sim 195$ peak regions, as illustrated in the bottom panel of Fig. 2, where the solar values are given by the shaded band. The correlations in each case are distinct, with different astrophysical conditions picking out different preferred values of V_0^p. Only the least negative values of V_0^p considered reproduce solar values for the high-entropy conditions, while values of V_0^p that tend towards the center of the distribution reproduce solar values for the low-entropy conditions. Within the range of values we consider, the fission recycling condi-

tions fail to reproduce solar values, with the correlation suggesting an even more negative value of V_0^p. Thus, if V_0^p could be more tightly constrained, the simulated ratio of the rare earth and $A \sim 195$ peak regions could be used as a diagnostic of r-process conditions.
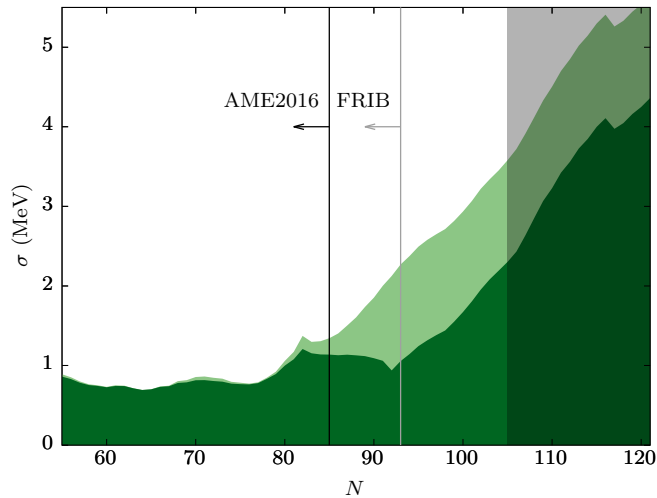

FIG. 3: Variations σ among our set of 50 UNEDF1 mass tables (light green shaded region) and our set of simulated mass tables (dark green shaded region), each with respect to the nominal UNEDF1 masses, for the tin isotopes. The AME2016 range of known masses [28] and anticipated FRIB reach are indicated, respectively, by black and gray solid lines. The vertical darkened band indicates the range in location for the one-neutron dripline.

Measurements of the masses of increasingly neutron-rich nuclei are the focus of a number of experimental efforts worldwide, for example at the Canadian Penning Trap at CARIBU [42, 43], JYFLTRAP at Jyväskylä [44, 45], ISOLTRAP at CERN [46], TITAN at TRIUMF [47], and storage rings at GSI in Germany, IMP in China, and RIKEN in Japan [48]. Next-generation radioactive ion facilities, such as the Facility for Rare Isotope Beams (FRIB), will have unprecedented access to isotopes far from stability [49]. New mass measurements improve the reliability of r-process simulations in two ways: directly, by dramatically reducing the uncertainty in the masses of newly measured nuclei, and indirectly, by enabling improvements to mass modeling. Theoretical mass models are all calibrated to known data, so known masses tend to be well reproduced by theory. Outside the known region, theoretical predictions tend to diverge. The variations among our fifty UNEDF1 mass tables, shown for the tin isotopes in Fig. 3, clearly demonstrate this behavior. For this element, UNEDF1 fits known masses to about $\sigma_{rms} \sim 1$ MeV, and variations increase sharply past the $N = 82$ closed shell. Additional measurements increase the available data with which to constrain theory and thus hold the potential to reduce uncertainties outside the measured region. We simulate this effect by

generating an adjusted set of fifty mass tables, in which the variations from the mean are reduced to match the experimentally-known region for nuclei within the FRIB range and increase with the same slope outside this range. The variations of the simulated set of tables are shown in the dark shaded region of Fig. 3.

Our two sets of UNEDF1 mass tables can be used to quantify the reductions in r-process abundance pattern uncertainties that have already been achieved by measurements to date and that are anticipated from future mass measurements. We rerun the example r-process simulations from Fig. 1 using three different sets of nuclear data. The first set is a theory-only set, with all quantities derived exclusively from our fifty UNEDF1 tables. The second set is that used in Fig. 1, where experimental nuclear data is additionally incorporated. The third set is constructed to mimic the influence of anticipated mass measurements. Experimental values or values derived from the nominal UNEDF1 mass tables are held fixed for all nuclei within the FRIB reach; elsewhere we use theory values derived from our set of fifty simulated UNEDF1 mass tables.
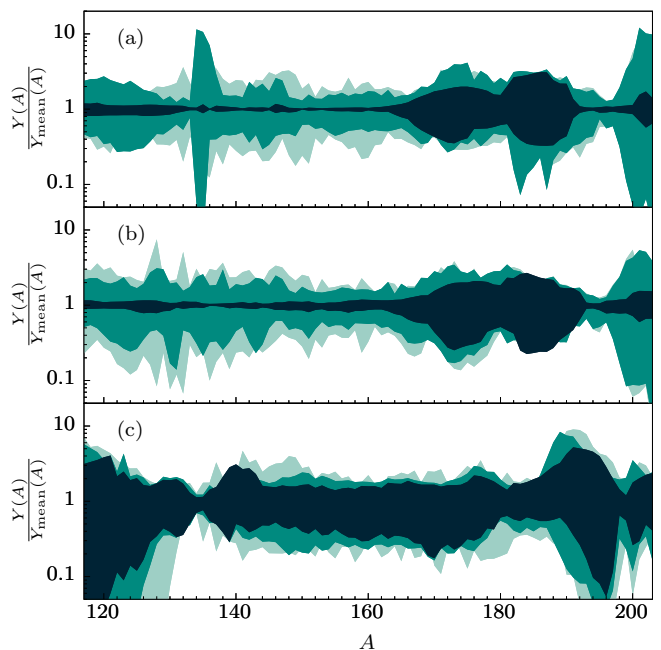

FIG. 4: Ratios of the abundances $Y(A)$ to the mean abundance $Y_{\mathrm{mean}}(A)$ for the set of fifty simulations with the example high entropy wind (top panel, (a)), low entropy wind (middle panel, (b)), and fission recycling outflow (bottom panel, (c)) astrophysical conditions, as in Fig. 1. The light shaded band shows theory-only calculations, the medium shaded band implements AME2016 masses and NUBASE2016 decay properties where available, and the dark shaded band additionally includes the simulated mass tables described in the text.

Fig. 4 shows the abundance pattern variations normal-

ized by the mean for the three astrophysical trajectories in Fig. 1, each calculated with the three data sets described above. For the high entropy wind, Fig. 4(a), many of the relevant nuclear properties have already been measured, so there is significant improvement realized between the theory-only (lightest shaded band) calculations and those that include current experimental values (medium shaded band). Looking forward to FRIB, the majority of nuclei along the equilibrium r-process path in the $N = 82$ and rare earth regions will be within reach. Thus systematic measurement campaigns at FRIB have the potential to essentially remove mass as a source of uncertainty in simulated r-process abundances below $A \sim 170$ for high entropy winds.

However, in the currently-favored potential $r-$process astrophysical site of neutron star/neutron star-black hole mergers, the environments are likely lower entropy, $s/k \sim 5 - 50$, and more neutron-rich, similar to the conditions used for the middle and bottom panels of Figs. 1 and 4. The r-process equilibrium paths are farther from stability in these cases, thus the current reach of experimental data results in more modest improvements, as indicated when comparing the light- and medium-shaded bands in Fig. 4(b) and (c). Prospects for the future, however, are encouraging. For the low-entropy wind example of Fig. 4(b), FRIB can reach the majority of the key nuclei and the remaining uncertainty band should be similar to the high-entropy wind case. In particular the excellent precision anticipated for abundances $140 < A < 170$ can facilitate the use of the rare earth peak as a key r-process diagnostic [43, 50].

For the fission recycling example, uncertainties in the location of the drip line and in the fission properties of heavy nuclei near the drip line dominate the uncertainty bands. Even with FRIB at full power these uncertainties are unlikely to be resolved with direct measurements. Here nuclear theory will play a critical role. The simulated improvements to theory anticipated in our approach do result in a narrowing of the uncertainty band, as seen in a comparison between the medium- and dark-shaded bands of Fig. 4(c). Further potential improvements to nuclear EDF theory, e.g. [51], and its full application to the problem of fission, e.g. [52, 53], are not captured in our approach. Therefore, there remains the possibility for more significant improvements to the uncertainty band associated with fission-recycling conditions with concurrent advances in experiment and theory.

The origins of the heaviest elements have remained mysterious for decades. Thanks to concerted efforts in astrophysical modeling, spectroscopic observations, neutrino and nuclear experiment and theory, and, now, gravitational wave astronomy, a detailed understanding of r-process nucleosynthesis finally seems within reach. Still, further advances are needed in each of these areas. Here we have highlighted how careful quantification of nuclear physics uncertainties has the potential to provide crucial insight into r-process astrophysical conditions and the nuclear models themselves.

[1] E. M. Burbidge, G. R. Burbidge, W. A. Fowler, and F. Hoyle. Synthesis of the Elements in Stars. *Reviews of Modern Physics*, 29:547–650, 1957.

[2] A. G. W. Cameron. Nuclear Reactions in Stars and Nucleogenesis. *Chalk River Reports*, CRL-41, 1957.

[3] B. S. Meyer, G. J. Mathews, W. M. Howard, S. E. Woosley, and R. D. Hoffman. R-process nucleosynthesis in the high-entropy supernova bubble. *Astrophys. J.*, 399:656–664, November 1992.

[4] S. E. Woosley, J. R. Wilson, G. J. Mathews, R. D. Hoffman, and B. S. Meyer. The r-process and neutrino-heated supernova ejecta. *Astrophys. J.*, 433:229–246, September 1994.

[5] A. Arcones, H.-T. Janka, and L. Scheck. Nucleosynthesis-relevant conditions in neutrino-driven supernova outflows. I. Spherically symmetric hydrodynamic simulations. *Astron. Astrophys.*, 467:1227–1248, June 2007.

[6] T. Fischer, S. C. Whitehouse, A. Mezzacappa, F.-K. Thielemann, and M. Liebendörfer. Protoneutron star evolution and the neutrino-driven wind in general relativistic neutrino radiation hydrodynamics simulations. *Astron. Astrophys.*, 517:A80, July 2010.

[7] L. Hüdepohl, B. Müller, H.-T. Janka, A. Marek, and G. G. Raffelt. Neutrino Signal of Electron-Capture Supernovae from Core Collapse to Cooling. *Physical Review Letters*, 104(25):251101, June 2010.

[8] L. F. Roberts, S. Reddy, and G. Shen. Medium modification of the charged-current neutrino opacity and its implications. *Phys. Rev. C*, 86(6):065803, December 2012.

[9] Y. Hirai, Y. Ishimaru, T. R. Saitoh, M. S. Fujii, J. Hidaka, and T. Kajino. Enrichment of r-process Elements in Dwarf Spheroidal Galaxies in Chemo-dynamical Evolution Model. *Astrophys. J.*, 814:41, November 2015.

[10] A. P. Ji, A. Frebel, A. Chiti, and J. D. Simon. R-process enrichment from a single event in an ancient

dwarf galaxy. *Nature*, 531:610–613, March 2016.

[11] B. P. Abbott *et al.* Gw170817: Observation of gravitational waves from a binary neutron star inspiral. *Phys. Rev. Lett.*, 119:161101, Oct 2017.

[12] P. S. Cowperthwaite *et al.* The electromagnetic counterpart of the binary neutron star merger ligo/virgo gw170817. ii. uv, optical, and near-infrared light curves and comparison to kilonova models. *The Astrophysical Journal Letters*, 848(2):L17, 2017.

[13] M. Arnould, S. Goriely, and K. Takahashi. The r-process of stellar nucleosynthesis: Astrophysics and nuclear physics achievements and mysteries. *Physics Reports*, 450:97–213, September 2007.

[14] M. R. Mumpower, R. Surman, G. C. McLaughlin, and A. Aprahamian. *Progress in Particle and Nuclear Physics*, 86:86–126, January 2016.

[15] Michael Bender, Paul-Henri Heenen, and Paul-Gerhard Reinhard. Self-consistent mean-field models for nuclear structure. *Rev. Mod. Phys.*, 75(1):121, 2003.

[16] N. Schunck, J. D. McDonnell, D. Higdon, J. Sarich, and S. M. Wild. Uncertainty quantification and propagation in nuclear density functional theory. *Eur. Phys. J. A*, 51(12):1, 2015.

[17] D. Martin, A. Arcones, W. Nazarewicz, and E. Olsen. Impact of Nuclear Mass Uncertainties on the r Process. *Physical Review Letters*, 116(12):121101, March 2016.

[18] R. Surman, M. Mumpower, and A. Aprahamian. Uncorrelated Nuclear Mass Uncertainties and r-process Abundance Predictions. *Acta Physica Polonica B*, 47:673, 2016.

[19] M. Kortelainen, J. McDonnell, W. Nazarewicz, P. G. Reinhard, J. Sarich, N. Schunck, M. V. Stoitsov, and S. M. Wild. Nuclear energy density optimization: Large deformations. *Phys. Rev.*, C85:024304, 2012.

[20] Dave Higdon, Jordan D. McDonnell, Nicolas Schunck, Jason Sarich, and Stefan M Wild. A Bayesian Approach for Parameter Estimation and Prediction using a Computationally Intensive Model. *J. Phys.*, G42(3):034009, 2015.

[21] J. D. McDonnell, N. Schunck, D. Higdon, J. Sarich, S. M. Wild, and W. Nazarewicz. Uncertainty Quantification for Nuclear Density Functional Theory and Information Content of New Measurements. *Phys. Rev. Lett.*, 114:122501, 2015.

[22] R. Navarro Perez, N. Schunck, R. D. Lasseri, C. Zhang, and J. Sarich. Axially deformed solution of the Skyrme–Hartree–Fock–Bogolyubov equations using the transformed harmonic oscillator basis (III) HFBTHO (v3.00): A new version of the program. *Comput. Phys. Commun.*, 220(Supplement C):363, 2017.

[23] N. Schunck, J. Dobaczewski, J. McDonnell, J. Mor, W. Nazarewicz, J. Sarich, and M. V. Stoitsov. One-quasiparticle states in the nuclear energy density functional theory. *Phys. Rev. C*, 81(2):024316, 2010.

[24] Jochen Erler, Noah Birge, Markus Kortelainen, Witold Nazarewicz, Erik Olsen, Alexander M. Perhac, and Mario Stoitsov. The limits of the nuclear landscape. *Nature*, 486(7404):509, 2012.

[25] T. Kawano, R. Capote, S. Hilaire, and P. Chau Huu-Tai. *Physical Review C*, 94(1):014612, July 2016.

[26] M. R. Mumpower, T. Kawano, and P. Möller. Neutron-γ competition for β-delayed neutron emission. *Phys. Rev. C*, 94:064317, Dec 2016.

[27] P. Möller, J. R. Nix, and K.-L. Kratz. *Atomic Data and Nuclear Data Tables*, 66:131, 1997.

[28] Meng Wang, G. Audi, F. G. Kondev, W. J. Huang, S. Naimi, and Xing Xu. The AME2016 atomic mass evaluation (II). Tables, graphs and references. *Chinese Phys. C*, 41(3):030003, 2017.

[29] G. Audi et al. The nubase2016 evaluation of nuclear properties. *Chinese Physics C*, 41(3):030001, March 2017.

[30] M. R. Mumpower, T. Kawano, J. L. Ullmann, M. Krtika, and T. M. Sprouse. Estimation of M 1 scissors mode strength for deformed nuclei in the medium- to heavy-mass region by statistical Hauser-Feshbach model calculations. *Physical Review C*, 96(2):024612, August 2017.

[31] M. R. Mumpower, T. Kawano, T. M. Sprouse, N. Vassh, E. M. Holmbeck, R. Surman, and P. Mller. β-delayed Fission in r-process Nucleosynthesis. *The Astrophysical Journal*, 869(1):14, December 2018.

[32] Erika M. Holmbeck, Trevor M. Sprouse, Matthew R. Mumpower, Nicole Vassh, Rebecca Surman, Timothy C. Beers, and Toshihiko Kawano. Actinide Production in the Neutron-rich Ejecta of a Neutron Star Merger. *The Astrophysical Journal*, 870(1):23, December 2018.

[33] Joel de Jesús Mendoza-Temis, Meng-Ru Wu, Karlheinz Langanke, Gabriel Martínez-Pinedo, Andreas Bauswein, and Hans-Thomas Janka. Nuclear robustness of the r process in neutron-star mergers. *Phys. Rev. C*, 92:055805, Nov 2015.

[34] C. Sneden, J. J. Cowan, and R. Gallino. Neutron-Capture Elements in the Early Galaxy. *Annual Review of Astronomy and Astrophysics*, 46:241–288, September 2008.

[35] M. R. Mumpower, G. C. McLaughlin, R. Surman, and A. W. Steiner. Reverse engineering nuclear properties from rare earth abundances in the r process. *Journal of Physics G Nuclear Physics*, 44(3):034003, March 2017.

[36] G.C. McLaughlin and R. Surman. Prospects for obtaining an r process from Gamma Ray Burst Disk Winds. *Nuclear Physics A*, 758:189–196, July 2005.

[37] R. Surman, G. C. McLaughlin, and W. R. Hix. Nucleosynthesis in the Outflow from Gamma-Ray Burst Accretion Disks. *The Astrophysical Journal*, 643(2):1057–1064, June 2006.

[38] O. Just, A. Bauswein, R. Ardevol Pulpillo, S. Goriely, and H.-T. Janka. Comprehensive nucleosynthesis analysis for ejecta of compact binary mergers. *Monthly Notices of the Royal Astronomical Society*, 448(1):541–567, March 2015.

[39] D. Martin, A. Perego, A. Arcones, F.-K. Thielemann, O. Korobkin, and S. Rosswog. Neutrino-driven winds in the aftermath of a neutron star merger: nucleosynthesis and electromagnetic transients. *The Astrophysical Journal*, 813(1):2, October 2015.

[40] Shinya Wanajo, Yuichiro Sekiguchi, Nobuya Nishimura, Kenta Kiuchi, Koutarou Kyutoku, and Masaru Shibata. Production of all the r-process nuclides in the dynamical ejecta of neutron star mergers. *The Astrophysical Journal*, 789(2):L39, June 2014.

[41] Daniel M. Siegel and Brian D. Metzger. Three-Dimensional General-Relativistic Magnetohydrodynamic Simulations of Remnant Accretion Disks from Neutron Star Mergers: Outflows and r -Process Nucleosynthesis. *Physical Review Letters*, 119(23):231102, December 2017.

[42] T. Y. Hirsh, N. Paul, M. Burkey, A. Aprahamian, F. Buchinger, S. Caldwell, J. A. Clark, A. F. Levand,

L. L. Ying, S. T. Marley, G. E. Morgan, A. Nystrom, R. Orford, A. P. Galván, J. Rohrer, G. Savard, K. S. Sharma, and K. Siegl. First operation and mass separation with the CARIBU MR-TOF. *Nuclear Instruments and Methods in Physics Research B*, 376:229–232, June 2016.

[43] R. Orford, N. Vassh, J. A. Clark, G. C. McLaughlin, M. R. Mumpower, G. Savard, R. Surman, A. Aprahamian, F. Buchinger, M. T. Burkey, D. A. Gorelov, T. Y. Hirsh, J. W. Klimes, G. E. Morgan, A. Nystrom, and K. S. Sharma. Precision Mass Measurements of Neutron-Rich Neodymium and Samarium Isotopes and Their Role in Understanding Rare-Earth Peak Formation. *Physical Review Letters*, 120(26):262702, June 2018.

[44] A. Kankainen, J. Hakala, T. Eronen, D. Gorelov, A. Jokinen, V. S. Kolhinen, I. D. Moore, H. Penttilä, S. Rinta-Antila, J. Rissanen, A. Saastamoinen, V. Sonnenschein, and J. Äystö. Isomeric states close to doubly magic ^{132}Sn studied with the double Penning trap JYFLTRAP. *Phys. Rev. C*, 87(2):024307, February 2013.

[45] M. Vilen, J. M. Kelly, A. Kankainen, M. Brodeur, A. Aprahamian, L. Canete, T. Eronen, A. Jokinen, T. Kuta, I. D. Moore, M. R. Mumpower, D. A. Nesterenko, H. Penttilä, I. Pohjalainen, W. S. Porter, S. Rinta-Antila, R. Surman, A. Voss, and J. ńystö. Precision Mass Measurements on Neutron-Rich Rare-Earth Isotopes at JYFLTRAP: Reduced Neutron Pairing and Implications for r -Process Calculations. *Physical Review Letters*, 120(26):262701, June 2018.

[46] D. Lunney and (on behalf of ISOLTRAP Collaboration. Extending and refining the nuclear mass surface with ISOLTRAP. *Journal of Physics G Nuclear Physics*, 44(6):064008, June 2017.

[47] D. Lascar, R. Klawitter, C. Babcock, E. Leistenschneider, S. R. Stroberg, B. R. Barquest, A. Finlay, M. Foster, A. T. Gallant, P. Hunt, J. Kelly, B. Kootte, Y. Lan, S. F. Paul, M. L. Phan, M. P. Reiter, B. Schultz, D. Short, J. Simonis, C. Andreoiu, M. Brodeur, I. Dillmann, G. Gwinner, J. D. Holt, A. A. Kwiatkowski, K. G. Leach, and J. Dilling. Precision mass measurements of $^{125-127}$Cd isotopes and isomers approaching the $N = 82$ closed shell. *ArXiv e-prints*, May 2017.

[48] Y. H. Zhang, Y. A. Litvinov, T. Uesaka, and H. S. Xu. Storage ring mass spectrometry for nuclear structure and astrophysics research. *Physica Scripta*, 91(7):073002, July 2016.

[49] https://groups.nscl.msu.edu/frib/rates/fribrates.html.

[50] M. R. Mumpower, G. C. McLaughlin, and R. Surman. Formation of the rare-earth peak: Gaining insight into late-time r-process dynamics. *Phys. Rev. C* , 85(4):045801, April 2012.

[51] L. Neufcourt, Y. Cao, W. Nazarewicz, and F. Viens. Bayesian approach to model-based extrapolation of nuclear observables. *Phys. Rev. C*, 98(3):034318, September 2018.

[52] S. A. Giuliani, G. Martínez-Pinedo, and L. M. Robledo. Fission properties of superheavy nuclei for r -process calculations. *Phys. Rev. C* , 97(3):034323, March 2018.

[53] A. Bulgac, S. Jin, K. Roche, N. Schunck, and I. Stetcu. Fission Dynamics. *arXiv e-prints*, June 2018.